iScience, Volume *25*

Supplemental information

Endothelial Shp2 deficiency controls alternative activation of macrophage preventing radiation-induced lung injury through notch signaling

Pan Liu, Yiqing Li, Mengyao Li, Hui Zhou, Huilun Zhang, Yuefei Zhang, Jiaqi Xu, Yun Xu, Jie Zhang, Bing Xia, Hongqiang Cheng, Yuehai Ke, and Xue Zhang

The supplementary data including supplementary figure 1-8 and the attached figure legends, primer lists for qRT-PCR, and human sample details.

Supplementary figures:

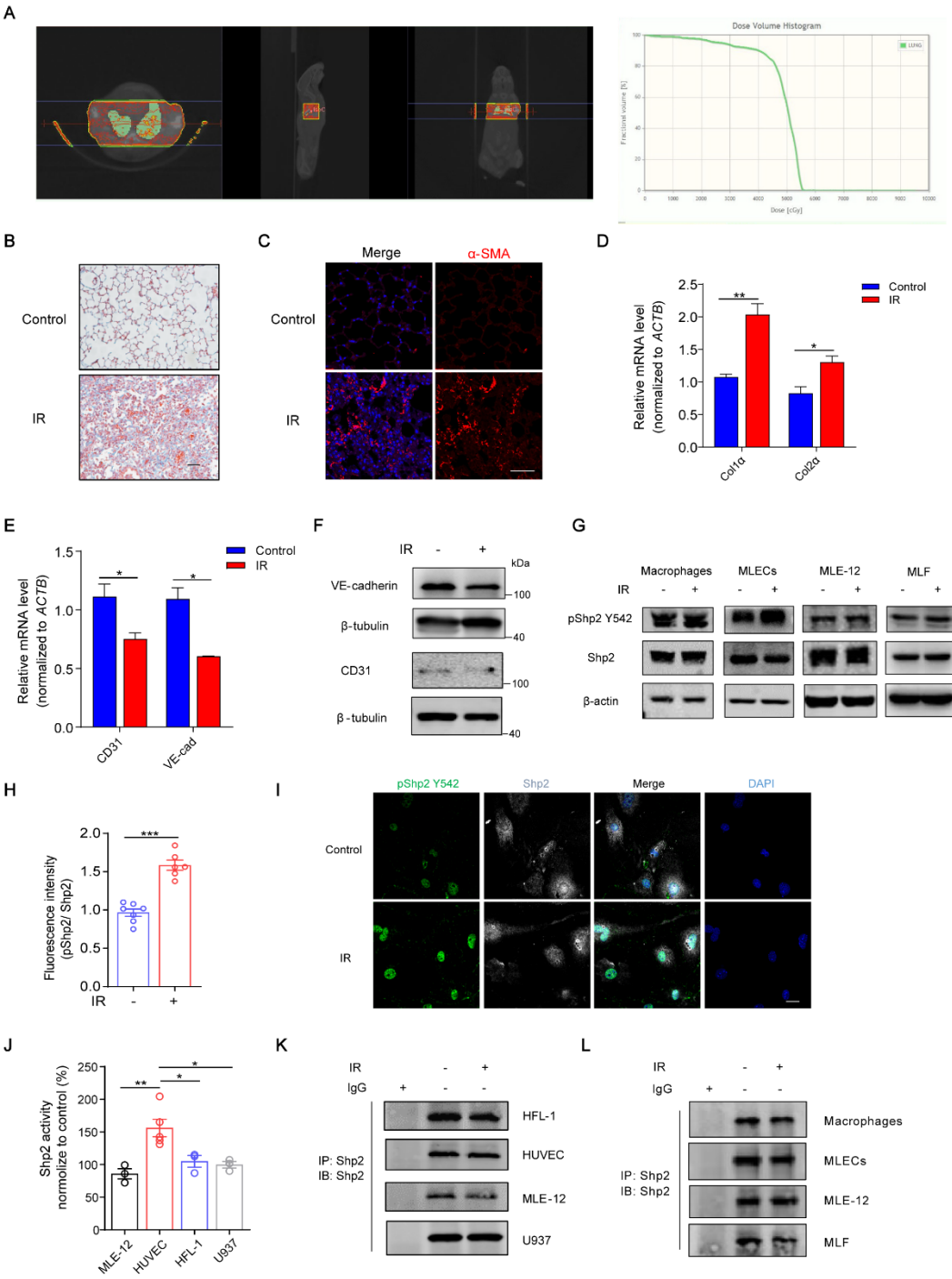

Figure S1. Phosphatase activity of Shp2 is upregulated in the mouse model of radiation-induced lung injury.

Related to Figure 1.

(A) Radiotherapy localization by thoracic CT scan. A single dose of 50 Gray was administered to the whole lung. (B, C) Lung sections from irradiated and control mice stained with Masson trichrome (B) α-SMA (red) and DAPI (blue) (C) to determine lung injury. Scale bar, 50 μm. (D) qRT-PCR analysis of relative Col1α and Col2α mRNA level in total lung RNA isolates. (E) qRT-PCR analysis of relative CD31 and VE-cadherin mRNA level in total lung RNA isolates. (F) Western blotting showing CD31 and VE-cadherin using proteins of whole lung lysates. β-tubulin was used as a loading control. (G) Representative western blotting images of total Shp2 and pShp2 Y542 in lysates of primary macrophages, endothelial cells (MLECs), epithelial cells (MLE-12), and fibroblasts (MLF). (H) The statistics graph of pShp2 Y542 fluorescence intensity in Figure 1H by ImageJ. (I) Immunofluorescence staining of pShp2 Y542 (red) and Shp2 (gray) in MLECs with or without irradiation. Nuclei were counterstained with DAPI (blue). Scale bar, 20 μm. (J) Phosphatase activity of Shp2 in lysates of HFL-1, HUVEC, MLE-12, and U937 cells measured by determining the hydrolysis of p-NPP. (K, L) Equal Shp2 was immunoprecipitated from cell lysates using a complex of protein A and Shp2 antibody to measure Shp2 activity. Data were shown as the mean± SEM of three independent experiments. *p< 0.05, **p< 0.01, ***p< 0.001

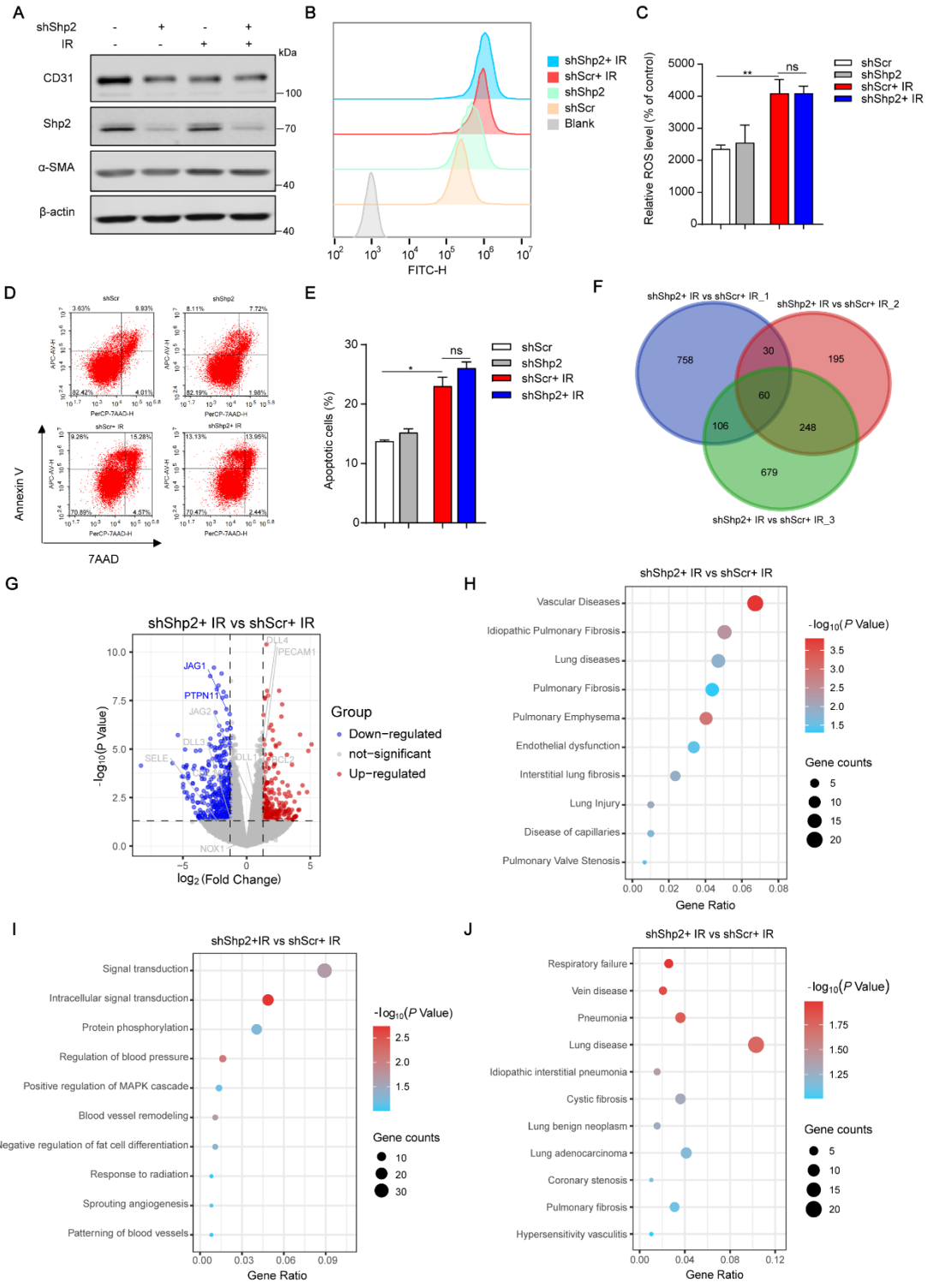

Figure S2. Radiation-induced endothelial dysfunction is independent of EndMT, ROS, and apoptosis in Shp2-deficient endothelium

Related to Figure 2.

(A) Western blotting showing expression level of endothelium (CD31) and mesenchymal cell

(α-SMA) markers in HUVECs lysates 48 h after irradiation (10 Gy), HUVECs were treated with shScr or shShp2 24 h before irradiation. (B) FCM analysis for ROS in HUVECs irradiated (10 Gy) for 40 min, then incubated with DCFH-DA (FITC, 10 μM) for 30 min. (C) Quantification of ROS normalized to control. (D) 7AAD/Annexin V determination of apoptotic cells 48 h after irradiation. (E) Counts of early and late stage apoptotic cells after irradiation. (F) Venn diagrams of differentially-expressed genes in three independent biological replicates of two conditions. (G) Volcano plot of genes differentially expressed in irradiated control and Shp2-deleted HUVECs (blue, downregulated genes; red, upregulated genes; fold-change< –1.3 or > 1.3, adjusted p-value< 0.05). (H) DisGeNET analysis of genes differentially expressed between irradiated control and Shp2-deletion HUVECs (DisGeNET pathways with *p*-value< 0.05 were enriched). (I) GO analysis of differentially-expressed genes (GO terms with *p*-value< 0.05 were enriched). (J) DO analysis of genes differentially-expressed between irradiated control and Shp2-deleted HUVECs; DO pathways with *p*-value< 0.05 were enriched. Data were shown as the mean± SEM of three independent experiments. *p< 0.05, **p< 0.01

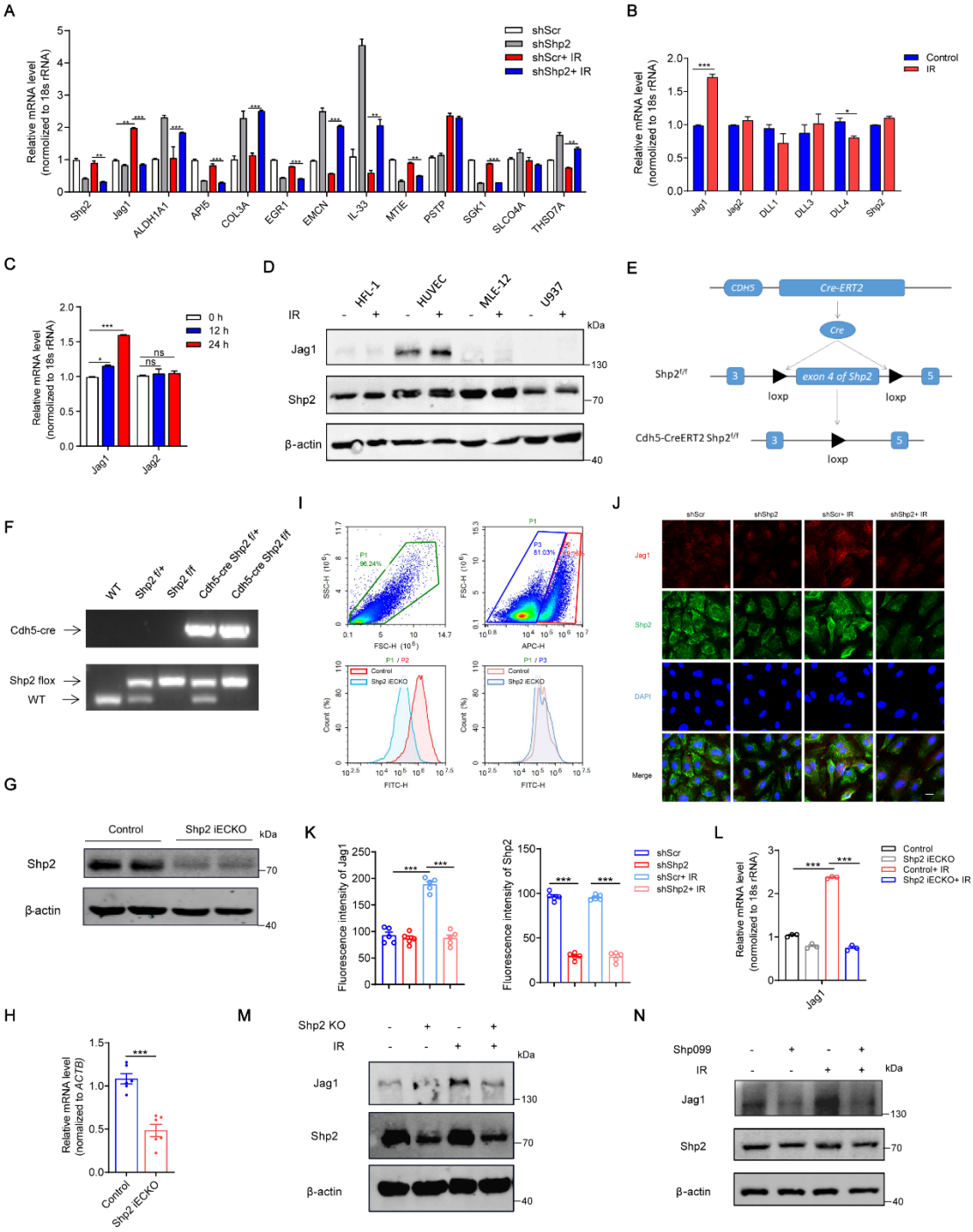

Figure S3. Shp2 deficiency blocks the radiation-induced Jag1 level.

Related to Figure 2.

(A) Relative mRNA levels of fibrosis-associated genes in HUVECs RNA isolates 24 h after irradiation. (B) qRT-PCR analysis of relative Notch ligands levels in HUVECs RNA isolates 24 h after irradiation. (C) qRT-PCR analysis of relative Jag1 and Jag2 levels in HUVECs RNA isolates 0, 12, 24 h after irradiation. (D) Western blotting showing Jag1 level in lysates of HFL-

1, HUVEC, MLE-12, and U937. β-actin was used as a loading control. Cells were irradiated with 10 Gy and then incubated for 48 h. (E) Generation of inducible endothelial-specific Shp2-deletion mice, cre-mediated deletion of exon 4 of Shp2 leaded to frameshift mutations. (F) Genotyping results of control and Shp2 iECKO mice. (G) Western blotting showing Shp2 level in MLECs lysates from control and Shp2 iECKO mice. β-actin was used as a loading control. (H) qRT-PCR analysis of relative Shp2 mRNA level in control and Shp2 iECKO MLECs. (I) FCM analysis of whole lung cells, the endothelial cells were defined as CD31 (APC) $^{+}$ events in the P2 window, other lung cells were defined as CD31 (APC) $^{-}$ events in the P3 window, the mean Shp2 (FITC) level in those cells were shown in the below pictures. (J) Immunofluorescence staining of Jag1 (red) and Shp2 (green) in HUVECs 48 h after irradiation. Nuclei were counterstained with DAPI (blue). Scale bar, 20 μm. ShShp2 lentivirus was administered to HUVECs 24 h prior to irradiation. (K) The statistics graph of Jag1 and Shp2 fluorescence intensity in (J) by ImageJ. (L) Relative Jag1 mRNA level were analyzed by qRT-PCR in MLECs 24 h after irradiation. (M) Jag1 levels were assessed by western blotting in MLECs 48 h after irradiation. β-actin was used as a loading control. (N) Western blotting showing Jag1 level using proteins of MLECs 48 h after irradiation. β-actin was used as a loading control. Shp099 (10 μM) was added to MLECs 2 h prior to irradiation. Data were shown as the mean± SEM of three independent experiments. *p< 0.05, **p< 0.01, ***p< 0.001

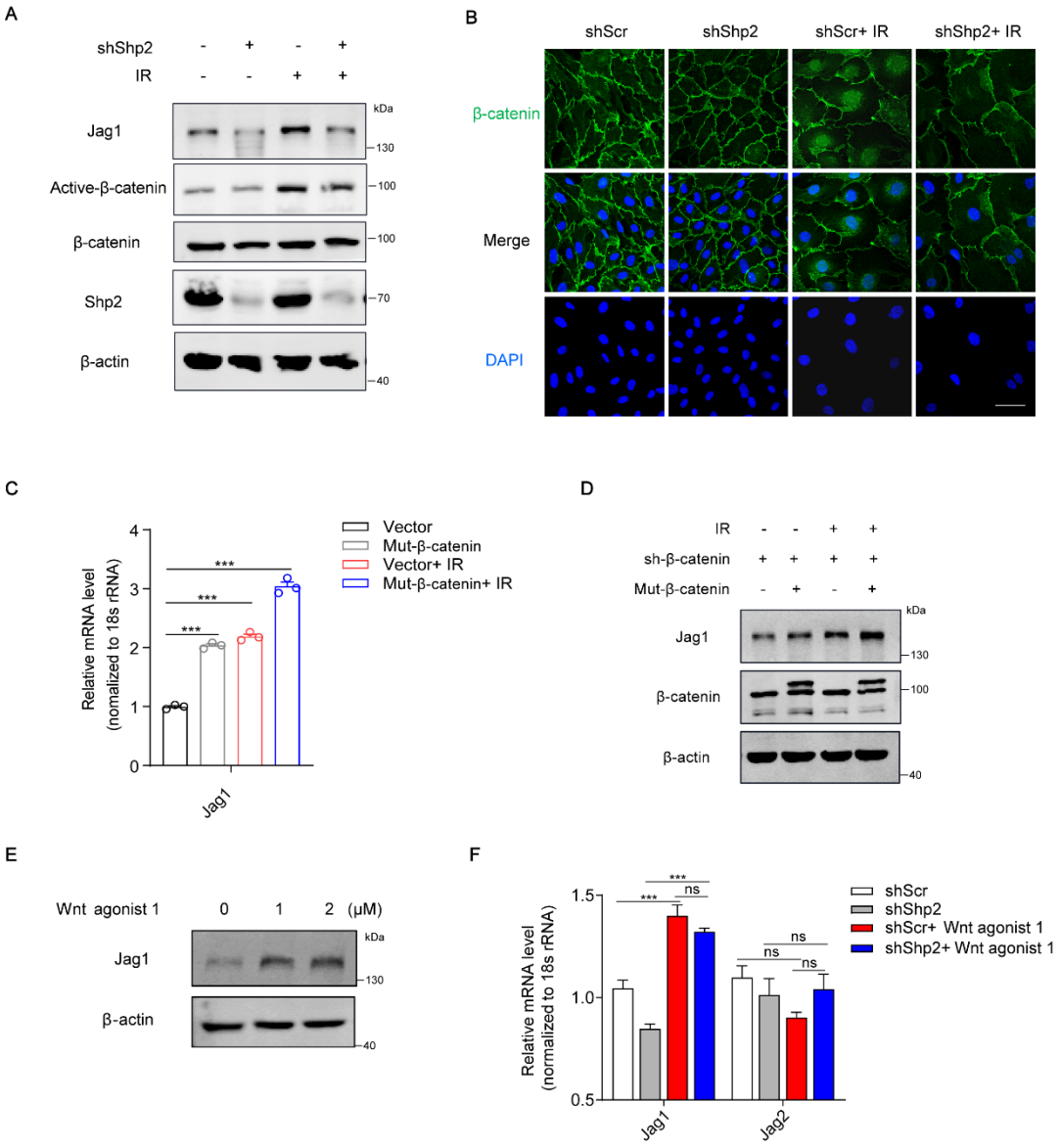

Figure S4. Shp2 deletion inhibits radiation-induced Jag1 expression *via* β-catenin pathway. Related to Figure 3.

(A) Western blotting showing total β-catenin and active-β-catenin level in Shp2-deleted HUVECs 6 h after irradiation. β-actin was used as a loading control. ShShp2 lentivirus was administered to HUVECs 36 h prior to irradiation. (B) Immunofluorescence staining of β-catenin (red) and Shp2 (green) in HUVECs 6 h after irradiation. Nuclei were counterstained with DAPI (blue). Scale bar, 50 μm. (C) Relative Jag1 mRNA levels were analyzed by qRT-PCR in HUVECs 24 h after irradiation. shβ-catenin lentivirus was administered to HUVECs, then mutant-β-catenin were added 24 h prior to irradiation. (D) Western blotting showing Jag1 level in HUVECs lysates. shβ-catenin lentivirus was administered to HUVECs 48 h after irradiation,

then mutant-β-catenin were added 24 h prior to irradiation. (E) Western blotting showing Jag1 level in HUVECs lysates. β-actin was used as a loading control. HUVECs were treated with Wnt agonist 1 (2 μM) for 24 h. (F) qRT-PCR analysis if relative Jag1 level in HUVECs RNA isolates. HUVECs were treated with shShp2 lentivirus for 36 h, and exposed to Wnt agonist 1 (2 μM) for 24 h after that. Data were shown as the mean± SEM of three independent experiments. $^{**}p< 0.01$, $^{***}p< 0.001$

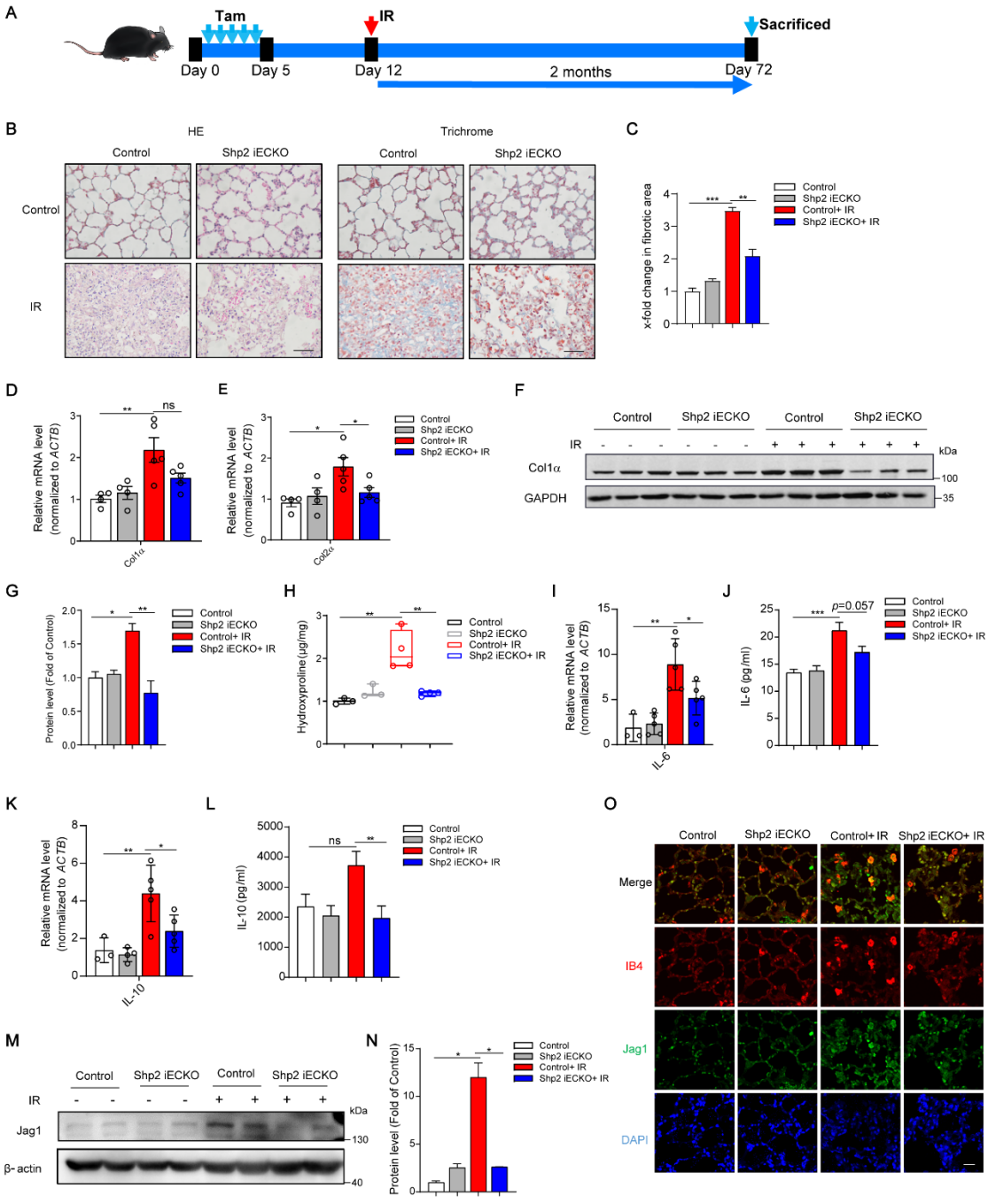

Figure S5. Shp2 deletion in endothelium reduces the radiation-induced Jag1 level in the radiation-induced lung injury model.

Related to Figure 4.

(A) Schematic illustrating the mouse model of radiation-induced lung injury. Shp2 iECKO and Control mice were injected with 20 mg/kg tamoxifen each day for 5 days, then subjected to thoracic irradiation with 50 Gy a week later. Lungs (n≥ 4) were harvested 2 months after irradiation. (B) Lung sections from Shp2 iECKO and control mice stained with H&E (left) or

Masson trichrome (right) to determine lung injury. Scale bar, 50 μm. (C) Fibrotic area in (B) from randomly-selected microscopic fields using ImageJ. (D, E) Relative Col1α and Col2α mRNA level were assessed in irradiated lungs (n≥ 4). (F) Col1α level were assessed by western blotting using proteins of whole lung lysates. GAPDH was used as a loading control. All samples were biologically independent and three independent experiments were performed. (G) Protein level of Col1α normalized to GAPDH in (F) were quantified by ImageJ. (H) Total hydroxyproline content of irradiated lungs from Shp2 iECKO and control mice. (I) Relative IL-6 level were assessed by qRT-PCR in irradiated control and Shp2 iECKO lungs. (J) IL-6 level in irradiated control and Shp2 iECKO BALF assessed by ELISA. (K) Relative IL-10 level were assessed by qRT-PCR in irradiated control and Shp2 iECKO lungs. (L) IL-10 level in irradiated control and Shp2 iECKO BALF assessed by ELISA. (M) Western blotting showing Jag1 level in irradiated lung lysates. β-actin was used as a loading control. (N) Protein level of Jag1 normalized to β-actin in (M) were quantified by ImageJ. (O) Immunofluorescence staining of Jag1 (green) and IB4 (red) in lung sections from irradiated mice. Nuclei were counterstained with DAPI (blue). Scale bar, 10 μm. Data were shown as the mean± SEM of three independent experiments. *p< 0.05, **p< 0.01, ***p< 0.001

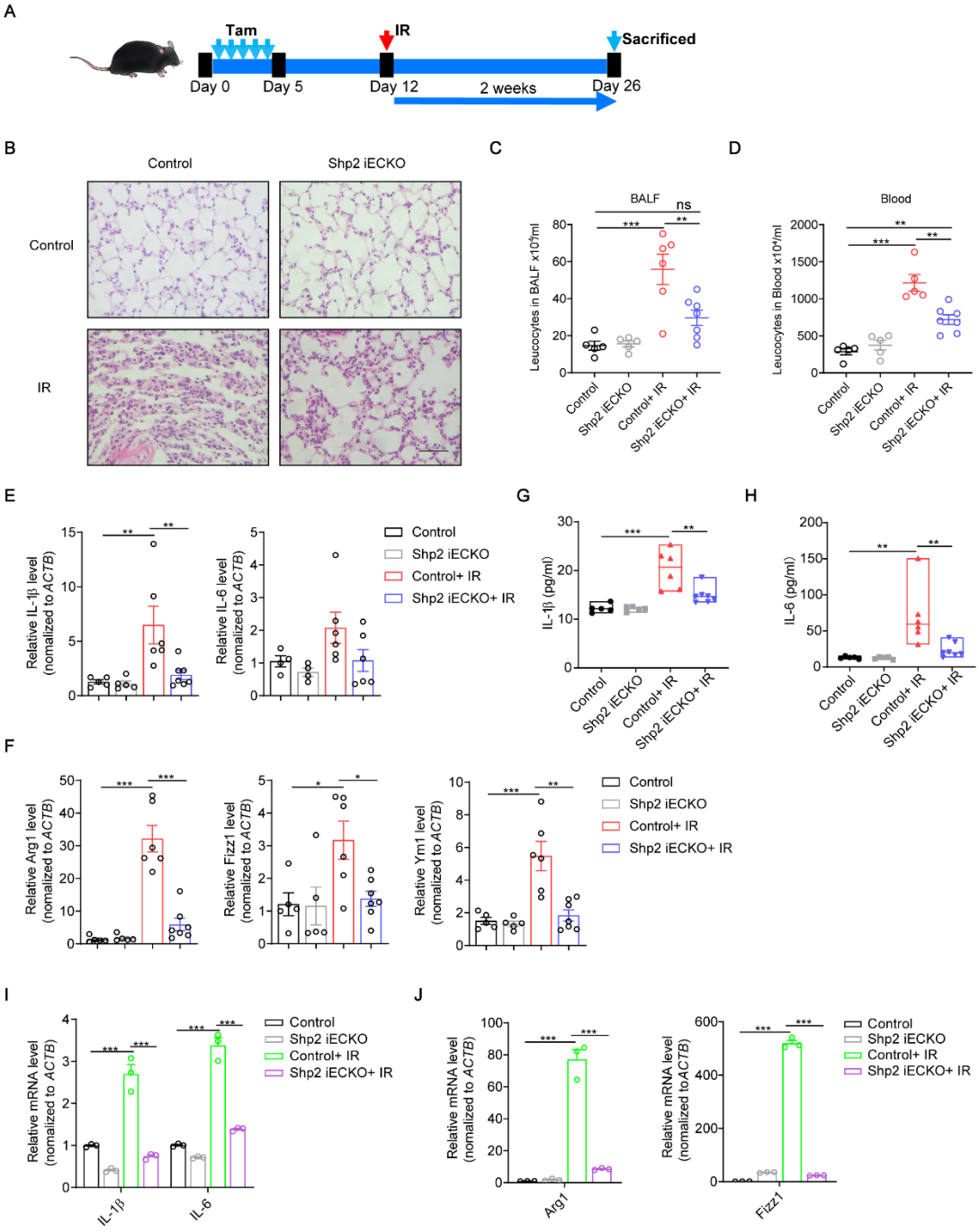

Figure S6. Shp2 deletion in endothelium reduces radiation-induced inflammation of lungs. Related to Figure 4, 5.

(A) Schematic illustrating the mouse model of radiation-induced lung injury. Shp2 iECKO and Control mice were injected with 20 mg/kg tamoxifen each day for 5 days, then subjected to thoracic irradiation with 50 Gy a week later. Lungs were harvested 2 weeks after irradiation. (n≥ 5) (B) Lung sections from Shp2 iECKO and control mice stained with H&E to determine lung injury. Scale bar, 50 μm. (C, D) Total leukocyte counts in BALF and blood from control and Shp2

iECKO mice with or without 50 Gy irradiation. (E) Relative IL-1β and IL-6 mRNA level were assessed by qRT-PCR in irradiated lungs (n≥ 5). (F) Relative Arg1, Fizz1 and Ym1 mRNA level were assessed by qRT-PCR in irradiated lungs (n≥ 5). (G, H) IL-1β and IL-6 level in irradiated control and Shp2 iECKO BALF were assessed by ELISA. (I) qRT-PCR analysis of relative IL-1β and IL-6 mRNA levels in AMs from the BALF of control and Shp2 iECKO mice 2 weeks after irradiation. (J) qRT-PCR analysis of relative Arg1, Fizz1, and Ym1 mRNA levels in AMs from the BALF of control and Shp2 iECKO mice 2 weeks after irradiation. Data were shown as the mean± SEM of three independent experiments. *p< 0.05, **p< 0.01, ***p< 0.001

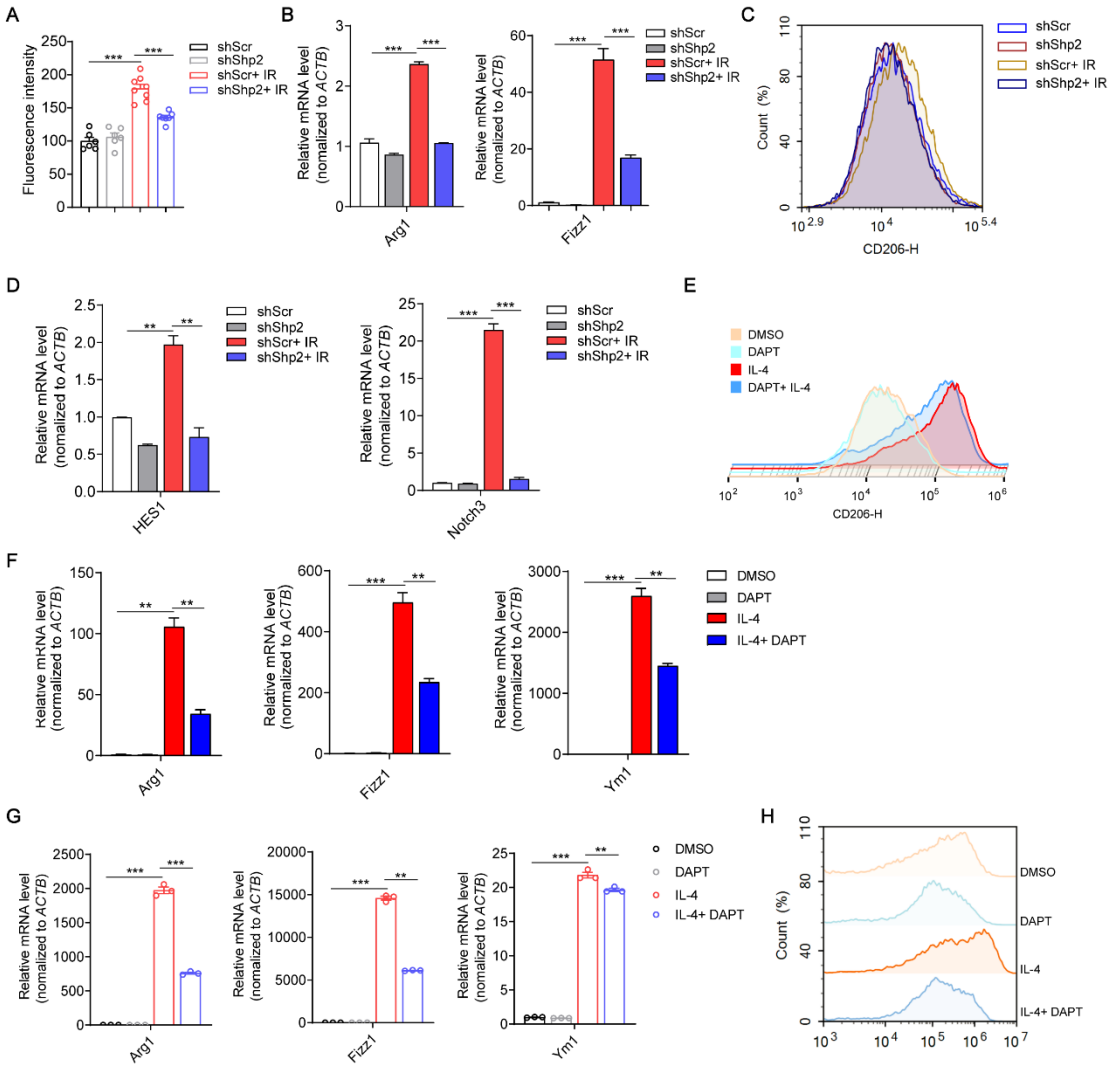

Figure S7. Endothelial Shp2 restrains M2-macrophage activation through Notch signaling. Related to Figure 6.

(A) The statistics graph of Arg1 fluorescence intensity in Figure 6B by ImageJ. (B) qRT-PCR analysis of relative Arg1 and Ym1 mRNA levels in BMDMs co-cultured with Shp2-deficient HUVECs for 24 h. (C) Expression of CD206 in BMDMs co-cultured with Shp2-deficient HUVECs for 24 h was determined by FCM. (D) qRT-PCR analysis of relative HES1 and Notch3 mRNA levels in BMDMs co-cultured with Shp2-deficient HUVECs for 24 h. (E) CD206 expression was determined by FCM in PMs treated with DAPT (20 μM) 2 h prior to IL-4 (20 ng/ml). (F) qRT-PCR analysis of relative Arg1, Fizz1, and Ym1 mRNA level in PMs, DAPT (20 μM) was added 2 h prior to IL-4 (20 ng/ml). (G) qRT-PCR analysis of relative Arg1, Fizz1, and Ym1 mRNA level in BMDMs, DAPT (20 μM) was added 2 h prior to IL-4 (20 ng/ml). (H) CD206 expression was determined by FCM in BMDMs treated with DAPT (20 μM) 2 h prior to IL-4 (20

ng/ml). Data were shown as the mean± SEM of three independent experiments. *p< 0.05, **p< 0.01, ***p< 0.001

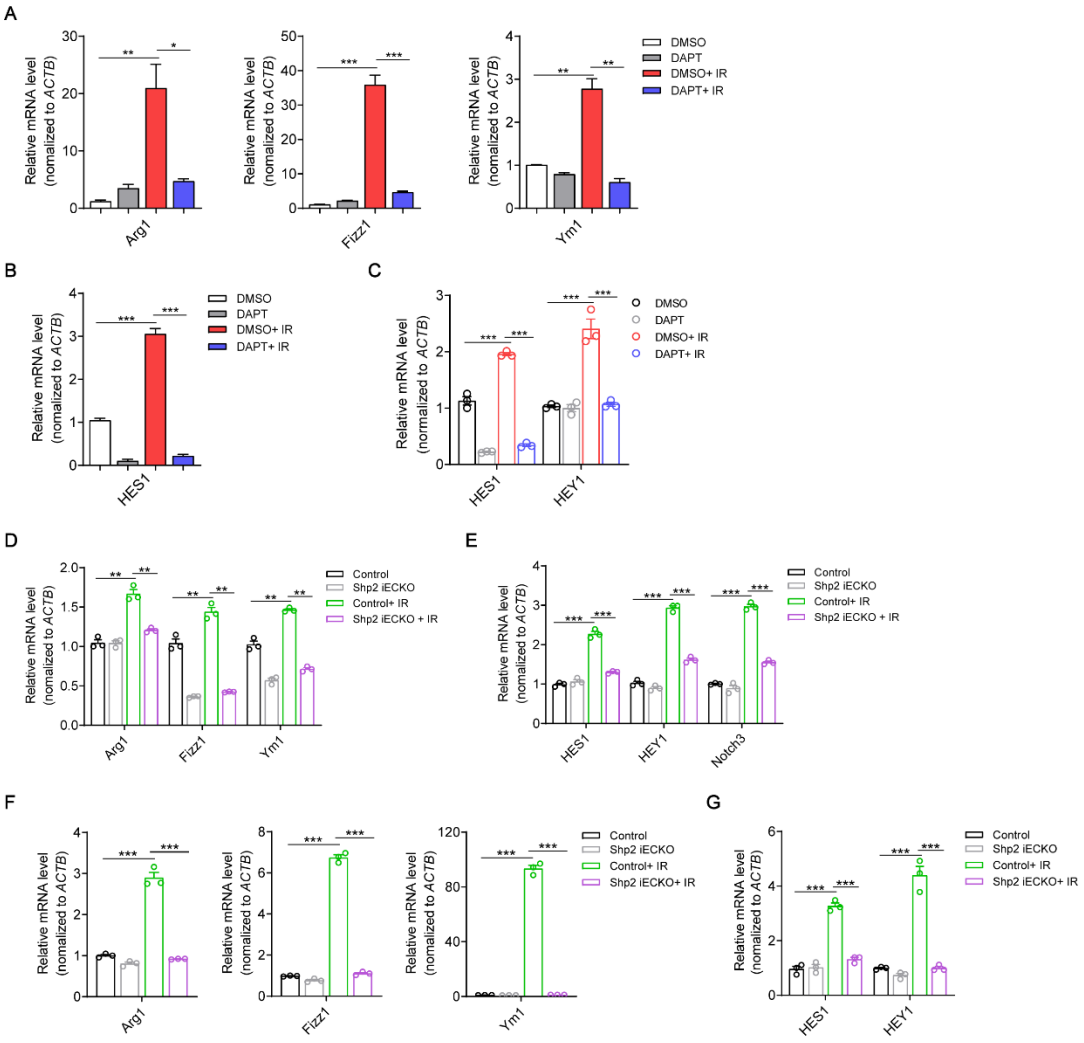

Figure S8. Shp2-deficient endothelium disrupts alternative activation of macrophage *via* Notch signaling

Related to Figure 6.

(A) qRT-PCR analysis of relative Arg1, Fizz1, and Ym1 mRNA levels in BMDMs co-cultured with irradiated HUVECs for 24 h, DAPT (20 μM) was added when co-culture started. (B) qRT-PCR analysis of relative HES1 mRNA level in BMDMs co-cultured with irradiated HUVECs for 24 h, DAPT (20 μM) was added when co-culture started. (C) qRT-PCR analysis of relative HES1 and HEY1 mRNA levels in PMs co-cultured with irradiated HUVECs for 24 h, DAPT (20 μM) was added when co-culture started. (D) qRT-PCR analysis of relative Arg1, Fizz1, and Ym1 mRNA levels in PMs co-cultured with irradiated MLECs for 24 h. (E) qRT-PCR analysis of relative HES1, HEY1 and Notch3 mRNA levels in PMs co-cultured with irradiated MLECs for 24 h. (F) qRT-PCR analysis of relative Arg1, Fizz1, and Ym1 mRNA levels in PMs co-cultured

with MLECs isolated from irradiated mice for 24 h. (G) qRT-PCR analysis of relative HES1 and HEY1 mRNA levels in PMs co-cultured with MLECs isolated from irradiated mice for 24 h. Data were shown as the mean± SEM of three independent experiments. *p< 0.05, **p< 0.01, ***p< 0.001

number	Blood volume	Sampling date	Patient type
1	2ml	2021.1.6	Control
2	2ml	2021.1.6	Control
3	2ml	2021.1.6	Control
4	2ml	2021.1.6	Control
5	5ml	2021.1.26	Control
6	5ml	2021.1.27	IR
7	5ml	2021.1.28	Control
8	5ml	2021.1.28	Control
9	2ml	2021.1.28	Control
10	5ml	2021.1.29	IR
11	5ml	2021.1.29	IR
12	5ml	2021.1.29	Control
13	5ml	2021.2.3	IR
14	5ml	2021.2.4	Control
15	5ml	2021.2.5	IR
16	5ml	2021.2.5	IR
17	5ml	2021.2.5	IR
18	5ml	2021.2.5	IR
19	5ml	2021.2.5	Control
20	5ml	2021.2.8	IR
21	5ml	2021.2.8	IR
22	5ml	2021.2.8	IR
23	5ml	2021.2.8	IR
24	5ml	2021.2.8	IR
25	5ml	2021.2.8	IR
26	5ml	2021.2.8	Control
27	5ml	2021.2.8	Control
28	5ml	2021.2.9	Control
29	3ml	2021.2.9	IR
30	3ml	2021.2.9	Control
31	5ml	2021.2.9	IR
32	5ml	2021.2.9	IR
33	5ml	2021.2.9	IR
34	5ml	2021.2.9	IR
35	5ml	2021.2.9	IR
36	5ml	2021.2.9	IR
37	5ml	2021.2.10	IR
38	5ml	2021.2.24	IR
39	3ml	2021.2.25	Control
40	5ml	2021.3.8	Control

Table S1. Patients' details. Related to STAR methods.

Human jag1 Forward	GCCGAGGTCCTATACGTTGC
Human jag1 Reverse	CCGAGTGAGAAGCCTTTTCAA
Human jag2 Forward	TGGGACTGGGACAACGATAC
Human jag2 Reverse	AGTGGCGCTGTAGTAGTTCTC
Human dll1 Forward	GATTCTCCTGATGACCTCGCA
Human dll1 Reverse	TCCGTAGTAGTGTTCGTCACA
Human dll3 Forward	CGTCCGTAGATTGGAATCGCC
Human dll3 Reverse	TCCCGAGCGTAGATGGAAGG
Human dll4 Forward	TGGGTCAGAACTGGTTATTGGA
Human dll4 Reverse	GTCATTGCGCTTCTTGCACAG
Human arg1 Forward	TGGACAGACTAGGAATTGGCA
Human arg1 Reverse	CCAGTCCGTCAACATCAAAACT
Human fizz1 Forward	CCGTCCTCTTGCCTCCTTC
Human fizz1 Reverse	CTTTTGACACTAGCACACGAGA
Human mrc1 Forward	CTACAAGGGATCGGGTTTATGGA
Human mrc1 Reverse	TTGGCATTGCCTAGTAGCGTA
Human shp2 Forward	AAAGGGGAGAGCAATGACGG
Human shp2 Reverse	CTCCACCAACGTCGTATTTCA
Human 18s rRNA Forward	GTAACCCGTTGAACCCCATT
Human 18s rRNA Reverse	CCATCCAATCGGTAGTAGCG
Human il6 Forward	ACTCACCTCTTCAGAACGAATTG
Human il6 Reverse	CCATCTTTGGAAGGTTCAGGTTG
Mouse col1a2 Forward	GGTGAGCCTGGTCAAACGG
Mouse col1a2 Reverse	ACTGTGTCCTTTCACGCCTTT
Mouse col1a1 Forward	TAAGGGTCCCCAATGGTGAGA
Mouse col1a1 Reverse	GGGTCCCTCGACTCCTACAT
Mouse shp2 Forward	TCG CGG AGA TGG TTT CAC
Mouse shp2 Reverse	TGG ACT TGC CGT CGT TGC
Mouse CD31 Forward	ACCGGGTGCTGTTCTATAAGG
Mouse CD31 Reverse	TCACCTCGTACTCAATCGTGG
Mouse notch1 Forward	CCCTTGCTCTGCCTAACGC
Mouse notch1 Reverse	GGAGTCCTGGCATCGTTGG
Mouse notch2 Forward	CTGTGAGCGGAATATCGACGA
Mouse notch2 Reverse	ATAGCCTCCGTTTCGGTTGG
Mouse notch3 Forward	AGTGCCGATCTGGTACAACTT

Mouse notch3 Reverse	CACTACGGGGTTCTCACACA
Mouse notch4 Forward	CTCTTGCCACTCAATTTCCCT
Mouse notch4 Reverse	TTGCAGAGTTGGGTATCCCTG
Mouse hey1 Forward	GCCCTGGCTATGGACTATCG
Mouse hey1 Reverse	CGCTGGGATGCGTAGTTGT
Mouse hes1 Forward	TCAGCGAGTGCATGAACGAG
Mouse hesS1 Reverse	CATGGCGTTGATCTGGGTCA
Mouse *ACTB* Forward	GGCTGTATTCCCCTCCATCG
Mouse *ACTB* Reverse	CCAGTTGGTAACAATGCCATGT
Mouse arg1 Forward	CTCCAAGCCAAAGTCCTTAGAG
Mouse arg1 Reverse	AGGAGCTGTCATTAGGGACATC
Mouse fizz1 Forward	TACTTGCAACTGCCTGTGCTTACT
Mouse fizz1 Reverse	TATCAAAGCTGGGTTCTCCACCTC
Mouse ym1 Forward	TCTCTACTCCTCAGAACCGTCAGA
Mouse ym1 Reverse	GATGTTTGTCCTTAGGAGGGCTTC
Mouse jag1 Forward	ATGCAGAACGTGAATGGAGAG

Table S2. Primers for qRT-PCR. Related to STAR Methods.